890 J. Med. Chem. 2011, 54, 890–900
DOI: 10.1021/jm101341m

Journal of Medicinal Chemistry Article

Screening Multicomponent Reactions for X-Linked Inhibitor of Apoptosis-Baculoviral Inhibitor of Apoptosis Protein Repeats Domain Binder

Ilaria Monfardini,[†] Jui-Wen Huang,[‡] Barbara Beck,[†] Jason F. Cellitti,[‡] Maurizio Pellecchia,[‡] and Alexander Dömling*,[†]

[†]University of Pittsburgh, Biomedical Science Tower 3, 3501 Fifth Avenue, Pittsburgh, Pennsylvania 15261, United States, and
[‡]Sanford-Burnham Medical Research Institute, 10901 North Torrey Pines Road, La Jolla, California 92037, United States

Received November 3, 2010

We report a second example of a general reaction screening approach to discover low molecular weight inhibitors of protein protein interactions. On the basis of the known pharmacophore model of SMAC mimetics, we predicted several inhibitors based on four different multicomponent reactions. The predicted inhibitors were subsequently synthesized, tested, and found to bind to the antiapoptotic protein X-linked inhibitor of apoptosis protein (XIAP) and showed cellular activity. Also the compounds are currently not highly potent. They could form a starting point for future medicinal chemistry optimization.

Introduction

Inhibitors of apoptosis proteins (IAP[a]) are key regulators of apoptosis and are thus important new mechanism-based cancer targets.[1,2] IAPs negatively regulate caspases, the executioner of apoptosis by a selective protein protein interaction (PPI). Smac (second mitochondria-derived activator of caspases) is a naturally occurring antagonist of IAPs and can effectively antagonize the inhibition of several initiator and effector caspases. Smac can release the specific binding of both the Bir3 domain of XIAP (X-linked inhibitor of apoptosis) with caspase-9 and the linker region between Bir1 and Bir2 with caspase-3 and -7. The hotspot of this protein−protein interaction is the tetrapeptide motif AVPI (Ala-Val-Pro-Ile). Current strategies focus mostly on the design of AVPI mimetics that target the Bir3 domain;[3] however, Bir2 domain directed strategies have also been reported.[4] The differential importance of the two domains, however, is currently subject to controversies.[5] A major disadvantage of many currently described AVPI mimetics is that they retain a very high peptide-like character, thus reducing their propensity to be orally bioavailable.[6−11] In contrast, more druglike AVPI mimetics tend to have a considerably reduced affinity for XIAP.[7] Recently, both Genentech and Novartis launched AVPI mimetics into a phase I clinical trial; however, the chemical structure of the compounds have not been disclosed (Figure 1).[12−14] Typical examples of published XIAP antagonists and their activities are shown in parts a,[15] b,[16] c,[14] d,[7] e,[4] and f[17] of Figure 1.

Discovery/Design Strategy of AVPI Mimetics

Current AVPI mimetics have been designed and discovered mostly by peptidomimetic approaches.[3,6,12−15] We recently introduced a new complementary approach to discover protein−protein interaction antagonists based on structural information of the interface. Herein we propose to excavate the most buried amino acid from the PPI interface and to rename this amino acid side chain "ANCHOR". Next we impose this fragment on efficiently chemical-accessible scaffolds (multicomponent reaction chemistry, MCR) and create virtual libraries based on several MCR scaffolds. These compound libraries are then docked into the PPI interface whereby the compounds' "anchors" align with the protein "anchor" as a starting pose. Manual inspection of the docking results or automatic scoring functions is then used to choose compounds for synthesis and screening. This novel approach was recently validated by the discovery of several new classes of HDM2 and the first HDM4 antagonists, as well as by dual-action HDM2/4 antagonists with high potency and cell activity.[18−20] Herein we describe our attempts to use the approach to discover XIAP antagonists.

Analyzing the X-ray structures available between XIAP and AVPI peptides, (e.g., PDB code 1TFQ) and the wealth of biochemical data, we chose the N-terminus of AVPI including the α-carbon and side chain of valine, not including the residual peptide as an essential fragment serving as an "anchor" endowed with initial affinity to XIAP (Figure 2).

The anchor residue then serves as a fragment for the generation of a virtual library of compounds based on different molecular scaffolds. These scaffolds were chosen from a database of several hundred multicomponent reactions (MCR) which provides high molecular diversity and fast and efficient chemistry to test our binding hypothesis.[21] To generate virtual libraries based on different MCR scaffolds, we used REACTOR from Chemaxon. This program supports "smart" reactions (generic reaction equations combined with reaction rules) generating chemically feasible products even in batch mode.[22] Thus, the fragment was imprinted onto different MCR scaffolds and for each scaffold several representatives were generated based on available starting materials for the corresponding MCR. Next these virtual libraries were docked into

*To whom correspondence should be addressed. Phone: 001-412-651-8425. Fax: 001-412-383-5298. E-mail: asd30@pitt.edu.

[a]Abbreviations: XIAP, X-linked inhibitor-of-apoptosis protein; IAP, inhibitor-of-apoptosis protein; BIR3, baculoviral inhibitor of apoptosis protein repeat; HSQC, heteronuclear single quantum coherence; FP, fluorescence polarization; ITC, isothermal titration calorimetry; AVPI, Ala-Val-Pro-Ile.

 Published on Web 01/11/2011

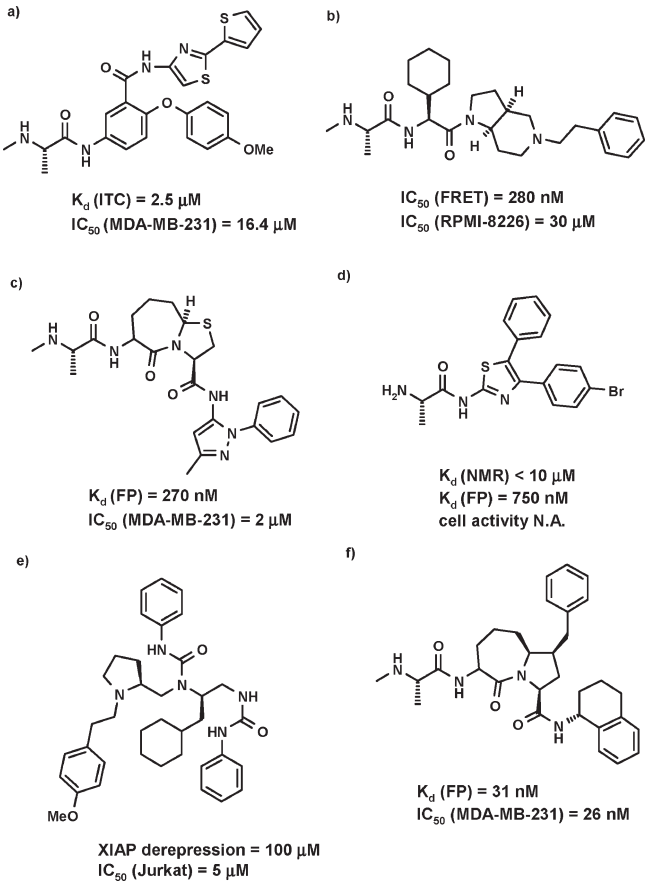

Figure 1. Representative XIAP antagonist classes.

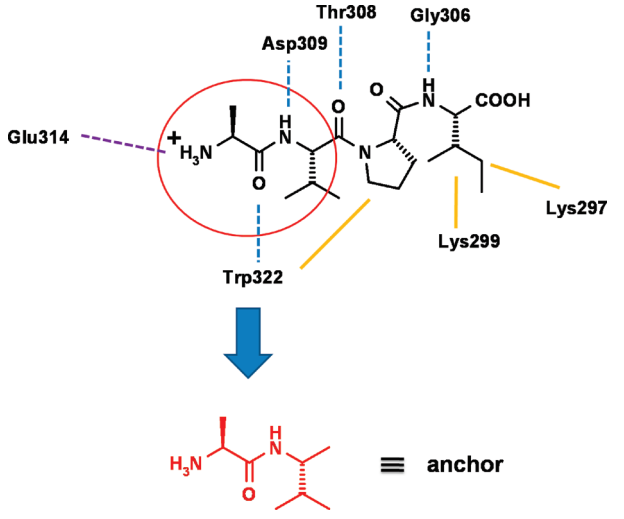

Figure 2. Schematic interaction between the tetrapeptide AVPI and XIAP (PDB code 1OWZ; AVPF bound to BIR3-XIAP). Hydrogen bonds are shown in blue, charge−charge interaction is shown in pink, and hydrophobic interactions are in yellow. The importance of the charge−charge interaction and the adjacent hydrogen bond network led us to define the Ala-Val dipeptide excluding the valine carbonyl as our anchor (shown in red).

the structure under a zero distance constraint regarding the fragment of the virtual library compounds and the Ala-Val fragment in the X-ray structure. As the modeling and docking suite, we used the software MOLOC.[23] The zero distance constraint was used to pose the compounds quickly and efficiently into a reasonable starting geometry and subsequently to optimize the compound. The target compounds for synthesis were chosen by the overall shape complementarities and the number and quality of proposed hydrogen bond interactions. According to this algorithm, we predicted several MCR scaffolds that looked promising as candidates to bind XIAP and were then chosen for further synthesis (Table 1). Typical docking poses for such predicted MCR compounds are shown in Figure 3.

Results and Discussion

Most currently known SMAC mimetics have a central moiety with an angle of $< 180°$ represented by Pro in the AVPI type peptides. This is an important feature, since it allows connecting the molecule parts addressing the Ala and Ile pockets in an efficient way. Our predicted scaffolds mimic this bending feature and therefore are based on four different MCRs and represent the heterocyclic backbones thiazolidine, (homo)piperazine, thiazole, and tetrazole (Table 1).

The rather complex structures incorporating a thiazoline as the proline mimetic can be convergent-synthesized by the combination of two MCRs, the well-known Asinger and the Ugi four-component condensation (Scheme 1).[24] The cyclic Schiff base thiazoline can be accessed in a great manifold by the MCR of α-haloaldehydes, sodium sulfide, ammonia, and oxo components, e.g., aldehydes or ketones.[29] The particular thiazolidine **5** was prepared from chloroacetaldehyde **1**, sodium hydrogen sulfide **2**, acetone **3**, and ammonia **4**.[30,31] The Asinger reaction yields the thiazoline in 70% yield as described in the literature. The subsequent Ugi reaction with diphenylmethyl isocyanide **7** and *N*-Boc protected Ala-Val dipeptide **6** yields after deprotection with TFA the target compound **9** in 22% yield over two steps.[24] Thus, a predicted XIAP binding molecule was synthesized in only three steps from commercially available starting materials. This synthetic approach can be potentially used to make derivatives in the central heterocyclic part, e.g., thiazolines with different substitution patterns or oxazolines or six-membered oxazines and thiazines.[32−36] In addition the isocyanide part and the dipeptide part should be amenable to straightforward variations.

The next scaffold contains a piperazine as a central cis-constrained moiety. Corresponding compounds **14** and **15** are quickly and efficiently accessible by a MCR involving mono-N-substituted ethylenediamines **10** and **11**, diphenyl isocyanide **7**, chloroacetaldehyde **1**, and a dipeptide derived carboxylic acid **6** (Scheme 2).[25,26] This reaction involves a Ugi reaction and an in situ nucleophilic substitution reaction of the intermediates **12** and **13**, respectively. Target compounds **14** and **15** were synthesized in only two steps according to this procedure followed by TFA mediated deprotection in quantitative and 56% yield, respectively.

Additionally we were interested in investigating the influence of the central ring size on the affinity to XIAP. Fortunately, simply by a switch to propylene diamines, the corresponding seven-membered diazepine **18** is accessible analogously, although in lower yield (Scheme 3).[27]

On the basis of these results, we predicted that compounds with a central thiazole moiety would also be of interest. Herein the thiazole nitrogen could potentially substitute the valine carbonyl and undergo similar hydrogen bonds. In addition the thiazole substitution pattern geometry seems to induce a steep enough angle to direct the carboxylic acid amide substituent into the hydrophobic subbinding site occupied by

Table 1. MCR Scaffolds with Predicted XIAP Bir3 Antagonistic Activity

	Reaction Scheme	Ref
1	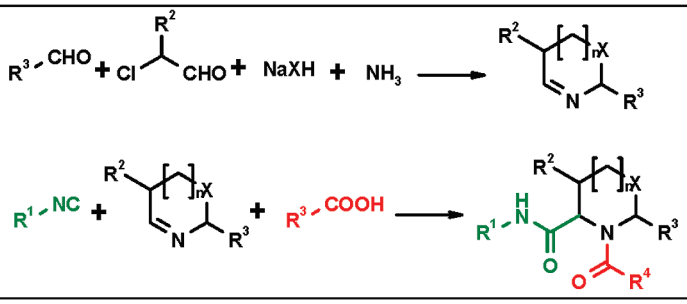	24
2	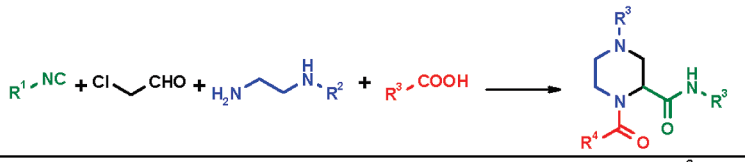	25,26
3	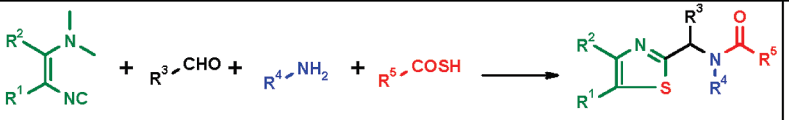	27
4	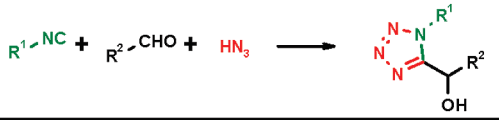	28

isoleucine in the tetrapeptide AVPI (Figure 1e). The thiazole MCR was introduced by us several years ago and proved to be very reliable and broad in scope.[27,37−41] It involves the reaction of a thiocarboxylic acid, a primary amine, an oxo component, and an isocyanide first described by Schöllkopf.[42] A target thiazole can be synthesized according to Scheme 4 in four steps from commercial starting materials. Boc-protected thioalanine **20** is made from the alanine precursor **19**.[43] Next, 2,4-dimethoxybenzylamine **22** is used as an ammonia substitute together with isobutyric aldehyde **21** and Schöllkopf's isocyanide **23** to yield thiazole **24** in 23% yield. We prepared **26** in 91% yield by a recently developed solventless direct conversion of methyl esters to amides,[44] which after TFA-mediated deprotection yields the target thiazole **27**.

Our modeling analysis suggests that a substitutent in the 5-position of the thiazole ring can potentially address the hydrophobic binding site on top of the Pro ring (Figure 3a,e). We synthesized the required phenyl substituted Schöllkopf isocyanide according to known procedures.[45] Analogous to the above and according to Scheme 5, we were able to synthesize thiazole target compound **34**.

The fourth backbone that was predicted to be active in binding to the AVPI site in XIAP was a hydroxymethyltetrazole amenable to synthesis by a tetrazole Passerini variant.[28] As a starting material, the Ala-Val dipeptide aldehyde **35** was required which was synthesized according to known procedures from dipeptide **6**.[46] Next, the Passerini reaction yielded the tetrazole target **39** after deprotection of **38** as a mixture of two diasteromers (Scheme 6). Interestingly, we were able to separate the two diastereomers at the stage of compound **38** by silica gel chromatography. However, acid deprotection yielded epimerization of the target compound **39**.

To test the binding activities of the predicted compounds to the Bir3 domain, we performed a fluorescence polarization primary assay. Initial screening of all compounds was carried out at 100, 10, 1, and 0.1 μM. For active compounds, six to seven point serial dilutions are made in duplicates. In order to exclude compounds with highly reactive bonds, which are likely to form covalent bonds, we look for changes in the IC_{50} in the presence of 1 mM Cys and/or 1 mM DTT. In addition, preincubation of inhibitor with the Bak-BH3 peptide before addition of Bcl protein and the resulting IC_{50} can give an indication of a fast and reversible binder. The result is summarized in Table 2. Clearly all of the predicted and tested compounds showed inhibition at the highest concentration measured (100 μM). Four compounds, however, also showed considerable activity at 1 μM or below. These are the piperazine **14**, the thiazoles **27** and **34**, and the tetrazole **39**. The IC_{50} of the best compound **14AB** in the TR-FRET assay was determined to be 4.9 μM (Figure 4).

To further establish the physical binding of the compounds to the Bir3 domain, we performed isothermal titration calorimetry (ITC) and 1D and 2D NMR experiments (Figure 5). Several compounds show considerably low micromolar affinity to the Bir3 domain, including **9**, **14**, and **15**.

Next the compounds were tested for their ability to induce apoptosis in cancer cells. We treated MDA-MB-231 cells with different compounds (Table 3). The MDA-MB-231 cell line was chosen because of its reported high inhibitor of apoptosis proteins (IAPs) expression levels and its sensitivity to Bir3 inhibitors.[47,48] Compound **15** can induce apoptosis at IC_{50} of 31 μM (Figure 6).

Conclusion

In summary, we aimed to discover several unprecedented XIAP binding AVPI mimicking scaffolds using the interplay of several techniques, including computational docking of the

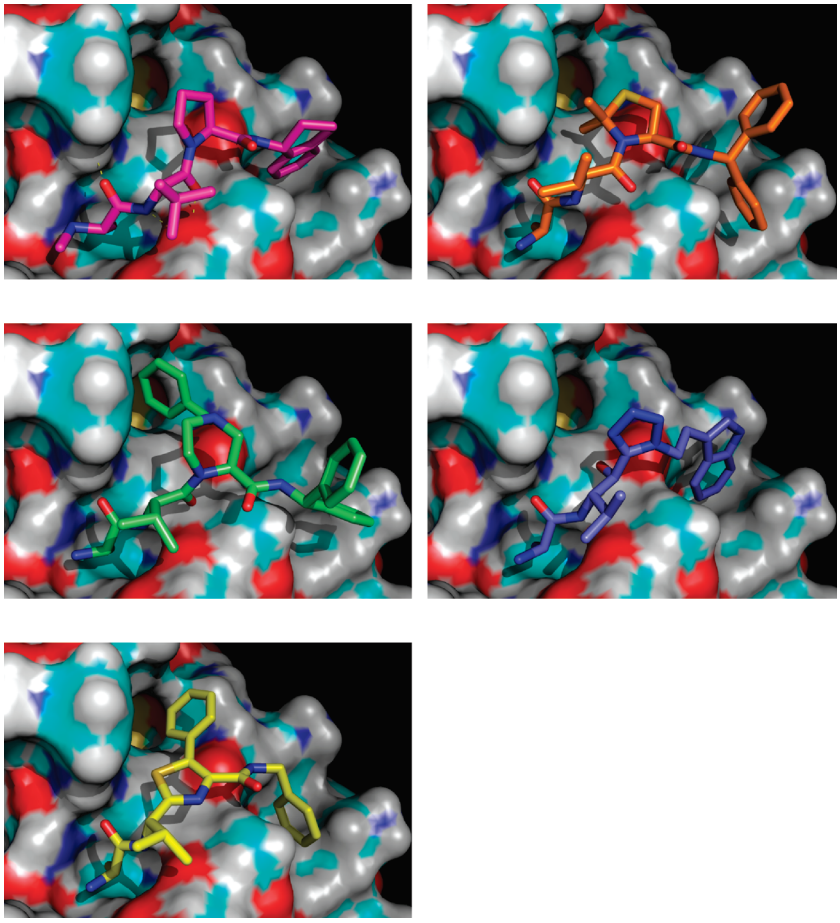

Figure 3. (a, upper left) X-ray structure of small molecular weight AVPI mimetic bound to XIAP (PDB code 1TFQ). The surface of XIAP is shown in gray. (a) The tetrapeptide mimetic is shown in pink rendered sticks. Hydrogen bond contacts are shown as yellow dotted lines. (b, upper right) Thiazoline AVPI mimetic **9** docking pose. (c, middle left) Piperazine AVPI mimetic **15** docking pose. (d, middle right) Tetrazole AVPI mimetic **38** docking pose. (e, lower left) Thiazole AVPI mimetic **32** docking pose. Pictures were rendered using PyMol.

Scheme 1. Synthesis of Thiazolidine Target **9**

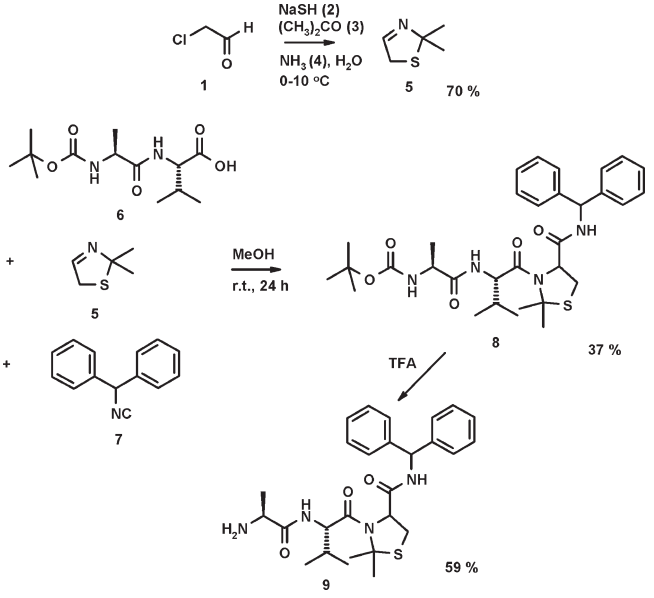

Scheme 2. Synthesis of Piperazine Targets **14** and **15**

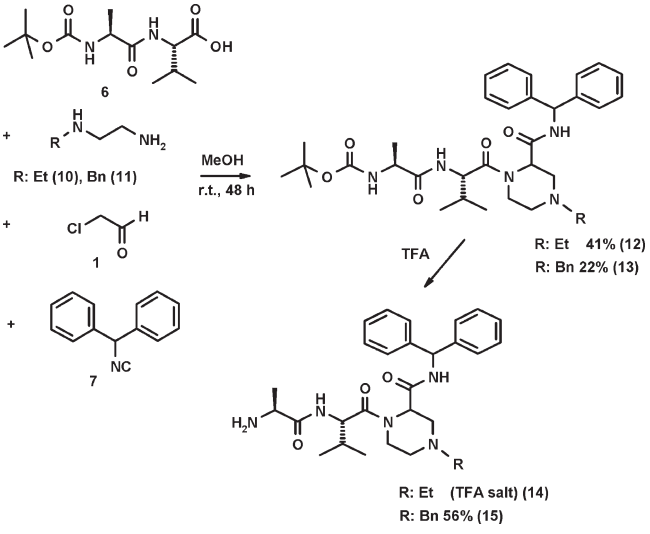

Ala anchor incorporating scaffold libraries from a MCR database, biophysical screening, and use of efficient and fast MCR chemistry. The goal of our study was to investigate if this method can deliver reasonable active compounds based on different scaffolds, which can serve as a starting point for further optimization. In fact several predicted and synthesized compounds are shown to bind in the micromolar range by several independent biophysical methods including NMR (HSQC), FP, and ITC assays. Additionally, compound **15** is cell-permeable and shows induction of apoptosis in the breast

Scheme 3. Synthesis of Homopiperazine Target **18**

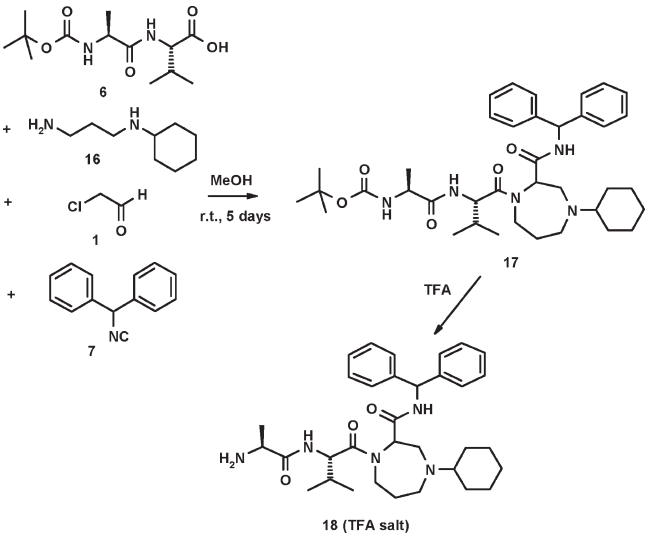

Scheme 4. Synthesis of Thiazole Target **27**

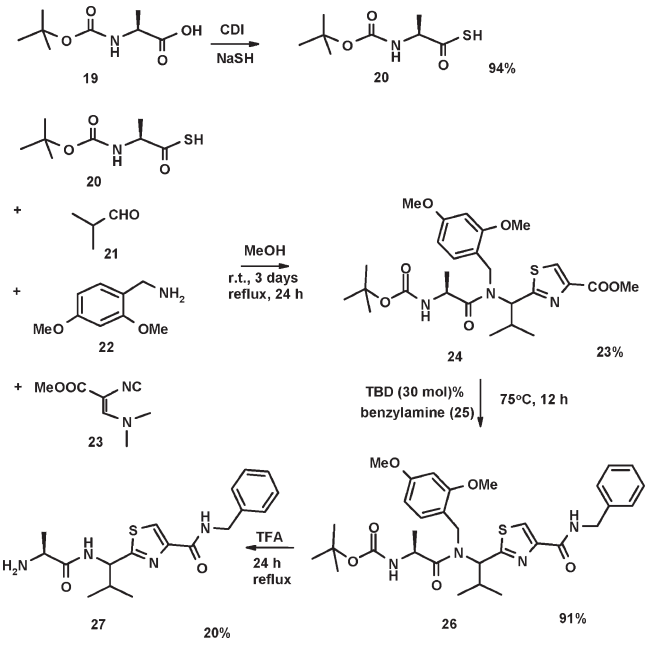

cancer cell line MDA-MB-231. Binding of the compound classes into the XIAP groove is rationalized using computational modeling. Further studies are needed to understand the structure−activity relationship as well as the mode of action of this lead series. Moreover, a wider variety of starting materials should lead to compounds with improved biological and pharmacokinetic activities.

The major method currently used to discover protein−protein interaction antagonist is high throughput screening (HTS). Whereas HTS campaigns in protein−protein interaction projects often yield very poor hit rates, the herein described process is more successful.[49,50] Recently, we showed the success of the method with p53/mdm2;[18] herein we show the method to work also with an unrelated protein−protein interaction XIAP(Bir3)/caspase-9. p53/Hdm2 is an α-helix mediated PPI with largely hydrophobic contacts.[51] The hot spot of XIAP/caspase-9, the tetrapeptide AVPI, however, shows a more diverse energetic interaction including charge−charge, hydrogen bonding, and hydrophobic interactions.

Scheme 5. Synthesis of Thiazole Target **34**

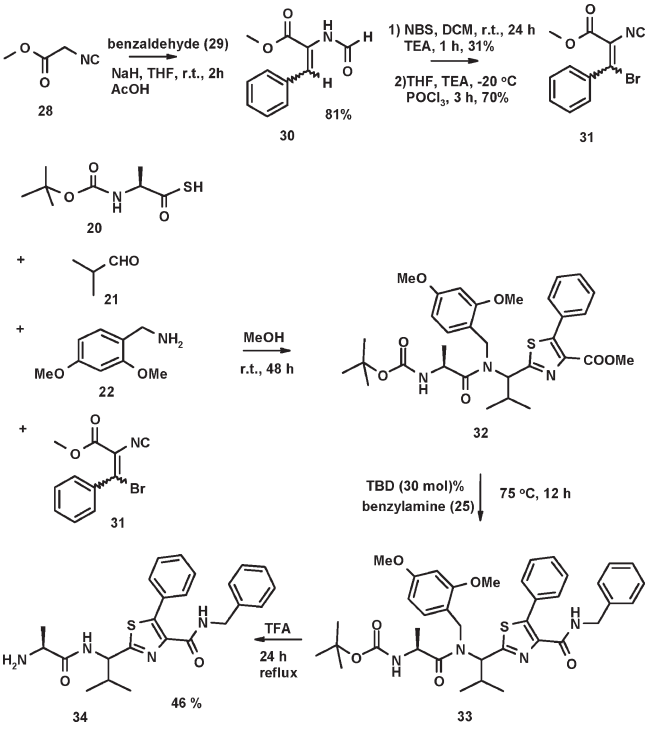

Scheme 6. Synthesis of Tetrazole Target **39**

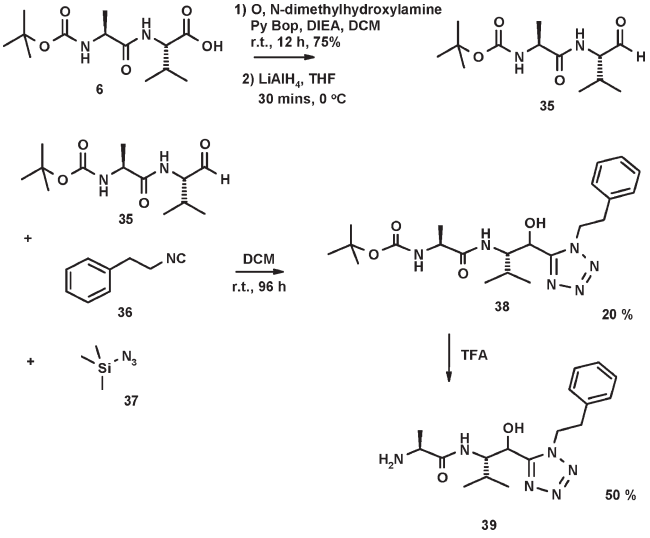

Table 2. TR-FRET Assay Results

	inhibition, %									
concn	**9**	**9A**	**9AB** (1/4)	**14**	**14A**	**15**	**18**	**27**	**34**	**39**	AVPI
100 μM	83.2	97.1	83.6	96.9	23.5	79.9	82.5	23.4	97.2	20.7	
10 μM	15.8	67.4	16.7	77.2		3.8	15.6	19.9	58.0	15.0	
1 μM				23.6				11.1	12.3	10.8	75.0
500 nM											55.4
100 nM				3.6					9.1		25.5

Our designed compounds presented herein have to be compared to the activities of the described compounds in Figure 1, with activities ranging from 100 μM to 31 nM. These are the results of a HTS campaign (Figure 1e) or extended optimization studies (Figure 1a−d,f). Clearly our compounds are far from being optimized and for all four predicted scaffolds only

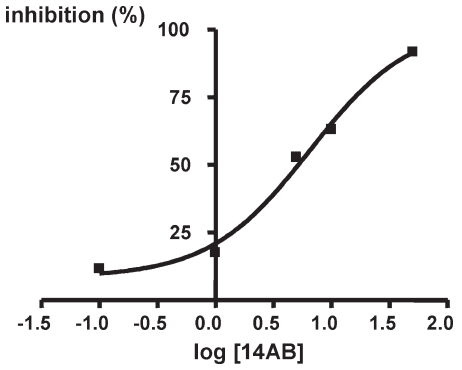

Figure 4. FP determined IC_{50} = 4.9 μM of **14AB**.

one or two derivatives were synthesized. The advantages of the current method are that several scaffolds can be potentially found as starting points for medicinal chemistry optimization based on efficient MCR chemistry. Parallel optimization of several backbones potentially reduces the preclinical attrition rate. In contrast to HTS, however, the current methods are dependent on structural information that is only available for a minority of PPIs.

Experimental Section

Chemistry. Standard syringe techniques were applied for transfer of air sensitive reagents and dry solvents. Solvents were purchased from Aldrich, Fisher Scientific, Acros Organics, and Alfa Aesar and used as received. ^{1}H and ^{13}C NMR spectra were recorded on Ultrashield Plus 600 and Bruker at 600 MHz and on Oxford 400 Varian at 400 MHz, respectively. Chemical shift values are in ppm relative to external TMS with high frequency shifts signed positive. Abbreviations used are as follows: s = singlet, d = doublet, m = multiplet, t = triplet, q = quartet. Data in parentheses are given in the following order: number of protons, multiplicity, and coupling constants in Hz. Flash chromatography was performed with the indicated solvent (mixture) and silica gel, MP Silitech 32−63 D, 60 Å, Bodman. Chromatotron chromatography was performed on Harrison Research chromatotron, serial no. 65F, with the indicated solvent (mixture) and silica gel, Merck, TLC grade 7749, with gypsium binder and fluorescent indicator, Sigma Aldrich. Thin layer chromatography was performed using Whatmann flexible-backed TLC plates on aluminum with fluorescence indicator. Compounds on TLC were visualized by UV or ninhydrin detection.

Purity (≥95%) of the compounds was determined by HPLC−MS measurements with Shimadzu Prominence UFLC (HPLC) and API 2000 LC/MS/MS systems and Applied Biosystems MDS SCIEX (MS) using water with 0.1% acetic acid and acetonitrile: gradient, 5−90% acetonitrile for 7 min; injection volume, 5 μL; detection wavelength, 254 nm.

***tert*-Butyl 1-(1-(4-(Benzhydrylcarbamoyl)-2,2-dimethylthiazolidin-3-yl)-3-methyl-1-oxobutan-2-ylamino)-1-oxopropan-2-ylcarbamate (8).** 2,2-Dimethyl-2,5-dihydrothiazole **5** (1 mmol, 155 mg) and the dipeptide BocAlaValOH **6** (1 mmol, 288 mg) are dissolved in 10 mL of MeOH. Diphenylmethyl isocyanide **7** (1 mmol, 193 mg) is added to the solution, and the mixture is stirred for 24 h at room temperature. The reaction mixture is concentrated under vacuum, diluted in EtOAc, and washed three times with 5% citric acid, three times with $NaHCO_3$, and once with brine. The organic layer is dried over Na_2SO_4 and evaporated under vacuum. The resulting crude is purified by column chromatography on silica gel with CH_2Cl_2/CH_3OH (99:1) to give a tan solid **8** (220 mg, 37%, diasteromeric ratio: 1:1). A subsequent column chromatography on silica gel with CH_2Cl_2/CH_3OH (99:1) affords separation between the two diastereomers. $C_{32}H_{44}N_4O_5S$ MW: 596.78 g/mol. HRMS (ESI-TOF) m/z $[M + Na]^+$: (calcd) 619.2930; (found) 619.2936. HPLC−MS t_R: 12.95 min. m/z $[M + H]^+$: 597.2.

Diastereomer A. ^{1}H NMR ($CDCl_3$, 600 MHz): δ = 0.88−1.02 (7H, m), 1.11−1.18 (2H, m), 1.45 (9H, s), 1.81 (3H, s), 1.84 (3H, s), 1.89−1.99 (1H, m), 3.20 (1H, q, J = 5), 3.61 (1H, d, J = 12), 4.02−4.10 (1H, m), 4.15−4.24 (1H, m), 4.67 (1H, s), 4.86 (1H,d, J = 5), 6.27 (1H, d, J = 7), 6.76 (1H, s), 7.16−7.41 (10H, m), 8.12 (1H, s). ^{13}C NMR ($CDCl_3$, 600 MHz): δ = 17.3, 19.7, 27.8, 28.4, 28.8, 32.3, 52.4, 57.4, 58.2, 66.7, 74.5, 127.4, 127.8, 128.4, 128.5,141.1, 169.3, 172.3.

Diastereomer B. ^{1}H NMR ($CDCl_3$, 600 MHz): δ = 0.55 (3H, d, J = 7) 0.72 (3H, d, J = 7), 1.32 (3H, d, J = 8), 1.42 (9H, s), 1.78−1.98 (7H, m), 3.16 (1H, d, J = 13), 3.43 (1H, q, J = 7), 4.12−4.18 (1H, m), 4.19−4.21 (1H, m), 4.93 (1H, s), 5.33 (1H, s), 6.23 (1H, d, J = 8), 6.62 (1H, s), 7.03−7.48 (11H, m). ^{13}C NMR ($CDCl_3$, 600 MHz): δ = 17.3, 19.3, 27.3, 28.3, 32.8, 52.1, 57.6, 57.9, 66.7, 74.4, 127.0, 127.6, 128.7, 128.9, 141.3, 158.9, 169.7.

3-((*S*)-2-((*S*)-2-Aminopropanamido)-3-methylbutanoyl)-*N*-benzhydryl-2,2-dimethylthiazolidine-4-carboxamide, Diastereomer A (9). In a 5 mL round-bottom flask is placed *tert*-butyl 1-(1-(4-(benzhydrylcarbamoyl)-2,2-dimethylthiazolidin-3-yl)-3-methyl-1-oxobutan-2-ylamino)-1-oxopropan-2-ylcarbamate **8** (0.03 mmol, 19 mg), and trifluoroacetic acid is added (100 μL). The solution is stirred for 10 min, and the trifluoroacetic acid residue is evaporated. A TLC plate DCM/MeOH 9:1 + 1% Et_3N on the crude gives a yellow solid **9** (9 mg, 59%). $C_{27}H_{36}N_4O_3S$, MW: 496.66 g/mol. HRMS (ESI-TOF) m/z $[M + Na]^+$: (calcd) 519.2406; (found) 519.2423. HPLC−MS t_R: 9.28 min. m/z $[M + H]^+$: 497.0. ^{1}H NMR ($CDCl_3$, 600 MHz): δ = 0.98 (3H, d, J = 7), 1.02 (3H, d, J = 7), 1.14 (3H, d, J = 7), 1.45−1.67 (2H, m), 1.83 (3H, s), 1.86 (3H, s), 1.95−2.04 (1H, m), 3.20 (1H, q, J = 6), 3.32 (1H, q, J = 6), 3.62−3.66 (1H, m), 4.14−4.21 (1H, m), 4.9 (1H, d, J = 5), 6.27 (1H, d, J = 8), 7.11−7.41 (10H, m), 7.71 (1H, s), 8.24 (1H, s).

3-((*S*)-2-((*S*)-2-Aminopropanamido)-3-methylbutanoyl)-*N*-benzhydryl-2,2-dimethylthiazolidine-4-carboxamide, Diastereomer B (9). In a 5 mL round-bottom flask is placed *tert*-butyl 1-(1-(4-(benzhydrylcarbamoyl)-2,2-dimethylthiazolidin-3-yl)-3-methyl-1-oxobutan-2-ylamino)-1-oxopropan-2-ylcarbamate **8** (0.05 mmol, 30 mg), and trifluoroacetic acid is added (100 μL). The solution is stirred for 10 min, and the trifluoroacetic acid residue is evaporated. A TLC plate DCM/MeOH 9:1 + 1% Et_3N on the crude gives a yellow solid **9** (5.4 mg, 21%). $C_{27}H_{36}N_4O_3S$, MW: 496.66 g/mol. HRMS (ESI-TOF) m/z $[M + Na]^+$: (calcd) 519.2406; (found) 519.2423. HPLC−MS t_R: 9.35 min. m/z $[M + H]^+$: 497.0. ^{1}H NMR ($CDCl_3$, 600 MHz): δ = 0.59 (3H, d, J = 7), 0.74 (3H, d, J = 7), 1.36 (3H, d, J = 7), 1.53−1.74 (2H, m), 1.81−1.98 (7H, m), 3.18 (1H, d, J = 13), 3.46 (1H, q, J = 7), 3.52−3.57 (1H, m), 4.11−4.19 (1H, m), 5.53 (1H, d, J = 7), 7.09 (1H, s), 7.21−7.44 (10H, m), 7.55 (1H, s).

***tert*-Butyl 1-(1-(2-(Benzhydrylcarbamoyl)-4-ethyl piperazin-1-yl)-3-methyl-1-oxobutan-2-ylamino)-1-oxopropan-2-ylcarbamate (12).** To a solution of *N*-ethylethylenediamine **10** (2 mmol, 210 μL) and BocAlaValOH **6** (2.12 mmol, 611 mg) in 2 mL of MeOH is added diphenyl isocyanide **7** (425 mg, 2.2 mmol) and aqueous chloroacetaldehyde solution **1** (4 mmol, 50% wt sol., 516 μL). The reaction mixture is stirred for 48 h at room temperature. The reaction mixture is diluted with EtOAc, washed three times with saturated $NaHCO_3$ solution and once with brine, dried, and evaporated. The resulting crude is purified by column chromatography on silica gel with EtOAc/MeOH 8:2 to give a tan solid **12** (490 mg, 41%, diastereomeric ratio: 1:1). $C_{33}H_{47}N_5O_5$, MW: 593.76 g/mol. HRMS (ESI-TOF) m/z $[M + H]^+$: (calcd) 594.3655; (found) 594.3608. HPLC−MS t_R: 9.15 min. m/z $[M + H]^+$: 593.8.

Diastereomer A. ^{1}H NMR ($CDCl_3$, 600 MHz): δ = 0.28−0.37 (3H, m), 0.95−1.05 (3H, m), 1.27−1.31 (3H, m), 1.36−1.53 (12H, m), 3.49−3.69 (1H, m), 3.69−3.95 (4H, m), 3.95−4.19

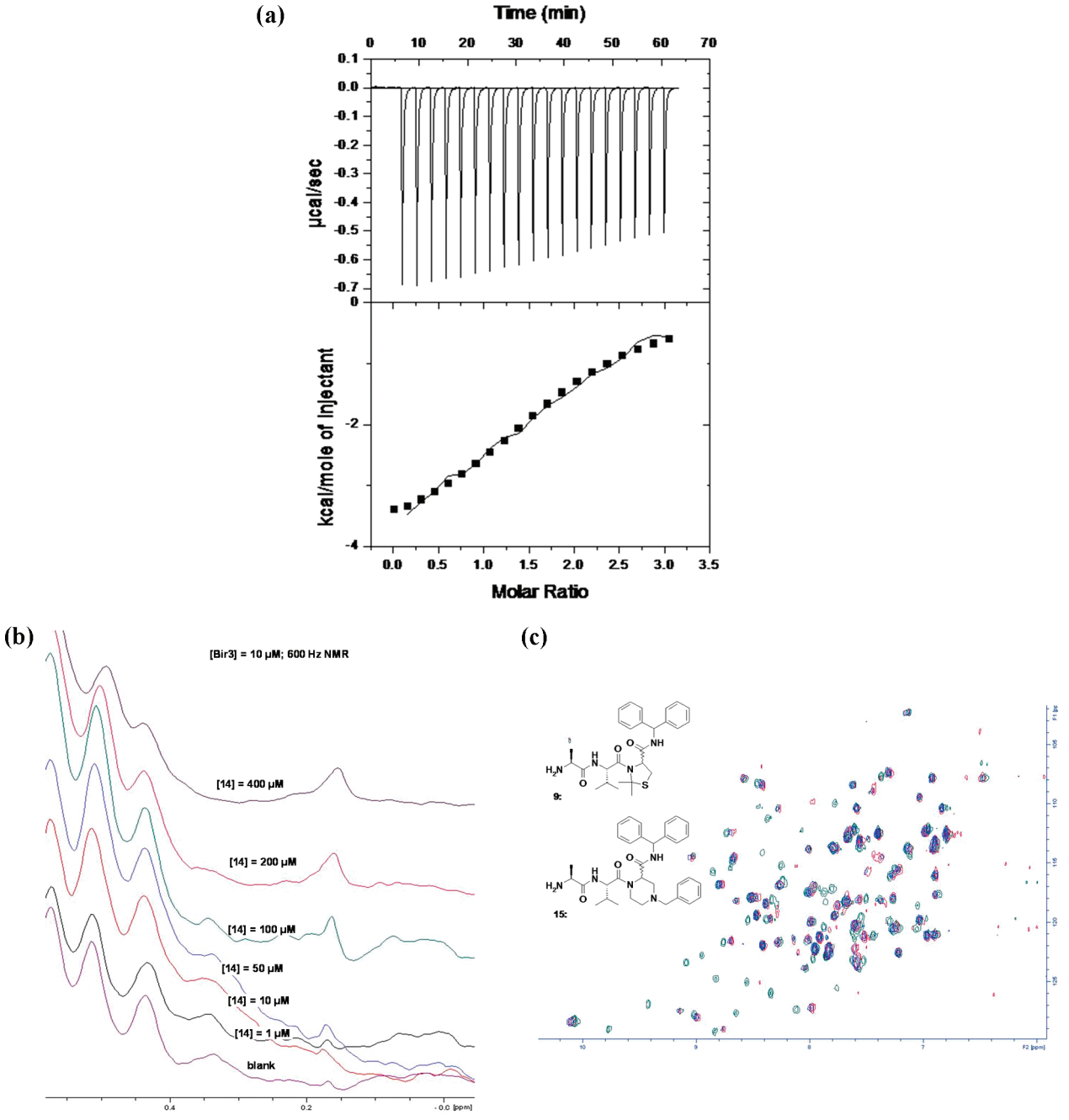

Figure 5. (a) Calorimetric titration of Bir3 with compounds **14** (a; K_d = 21.6 μM). The top panel shows raw data in power versus time. The bottom panel shows data after peak integration, subtraction of blank titration data, concentration normalization, and the fit to a single binding site model. (b) NMR titration of compound **14** to a 10 mM solution of Bir3. The experimental data were fitted to the nonlinear equation as described in the methods section, resulting in K_d = 27.7 μM. (c) HSQC NMR of 100 μM Bir3 (red) in H_2O phosphate buffer (50 mM, pH 7) and in the presence of 500 μM **9** (green) and 500 μM **15** (blue).

Table 3. Cell Viability Assay with MDA-MB-231 Breast Cells and Selected Compounds

IC$_{50}$, μM									
9	**15**	**14A**	**9A**	**9AB** (1/4)	**14**	**18**	**27**	**34**	**39**
> 50	31	> 50	> 50	> 50	> 50	38	> 50	> 50	> 50

(2H, m), 4.19−4.41 (2H, m), 4.41−4.66 (2H, m), 5.96−6.19 (2H, m), 7.13−7.24 (2H, m), 7.24−7.36 (4H, m), 7.36−7.46 (2H, m), 7.46−7.59 (2H, m), 9.70 (1H, s), 9.78 (1H, m). ^{13}C NMR ($CDCl_3$, 600 MHz): δ = 13.7, 18.4, 18.7, 20.6, 28.3,s 43.0, 44.6, 47.6, 50.8, 52.7, 57.4, 59.6, 60.2, 80.12, 127.1, 127.2, 127.8, 128.6, 140.9, 142.2, 155.7, 167.0, 167.3, 171.1, 175.2.

Diastereomer B. ^{1}H NMR ($CDCl_3$, 600 MHz): δ = 0.80−0.89 (3H, m), 0.93−1.01 (3H, m), 1.07−1.18 (3H, m), 1.26−1.37 (12H, m), 2.74−2.92 (1H, m), 3.06−3.19 (1H, m), 3.61−3.83 (3H, m), 3.83−4.06 (3H, m), 4.16−4.40 (1H, m), 4.58−4.72 (1H, m), 5.05−5.18 (1H, m), 5.80 (1H, s), 6.18 (1H, s), 7.10−7.66 (10H, m), 9.10 (1H, s), 9.96 (1H, m). ^{13}C NMR ($CDCl_3$, 600 MHz): δ = 14.2, 16.2, 19.5, 28.3, 29.3, 43.1, 44.5, 47.5, 49.3, 53.1, 57.2, 59.5, 60.3, 79.5, 126.7, 127.1, 127.8, 128.6, 141.1, 141.9, 154.8, 166.5, 167.7, 174.4.

1-((*S*)-2-((*S*)-2-Aminopropanamido)-3-methylbutanoyl)-*N*-benzhydryl-4-ethylpiperazine-2-carboxamide 2,2,2-Trifluoroacetate (14). In a 5 mL round-bottom flask is placed *tert*-butyl 1-(1-(2-(benzhydrylcarbamoyl)-4-ethylpiperazin-1-yl)-3-methyl-1-oxobutan-2-ylamino)-1-oxopropan-2-ylcarbamate **12** (0.16 mmol, 97 mg), and

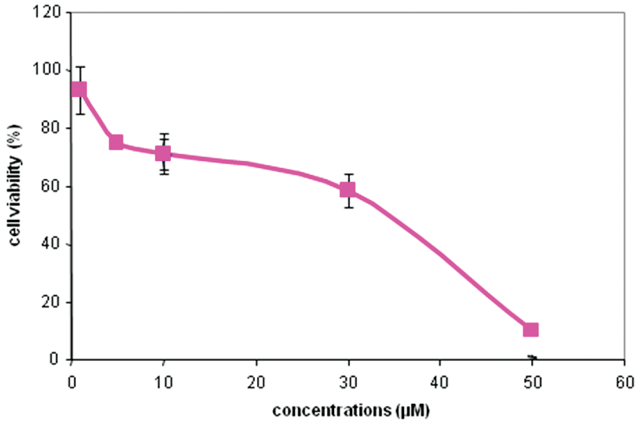

Figure 6. Concentration dependent cell viability of MDA-MB-231 breast cancer cells of **15**.

trifluoroacetic acid is added (200 μL). The solution is stirred for 10 min and the trifluoroacetic acid residue is evaporated to give a tan solid **14** (122 mg, quantitative yield). $C_{30}H_{40}F_3N_5O_5$, MW: 607.66 g/mol. HRMS (ESI-TOF) *m/z* $[M + H]^+$: (calcd) 494.3131; (found) 494.3119. HPLC−MS t_R: 7.93 min. *m/z* $[M + H]^+$: 494.2.

***tert*-Butyl 1-(1-(2-(Benzhydrylcarbamoyl)-4-benzyl piperazin-1-yl)-3-methyl-1-oxobutan-2-ylamino)-1-oxopropan-2-ylcarbamate (13).** To a solution of *N*-benzylethylenediamine **11** (1 mmol, 150 mg) and BocAlaValOH **6** (1.06 mmol, 305 mg) in 1.5 mL of MeOH are added diphenyl isocyanide **7** (212 mg, 1.1 mmol) and aqueous chloroacetaldehyde solution **1** (2 mmol, 50% wt sol., 258 μL). The reaction mixture is stirred at room temperature for 48 h. The reaction mixture is diluted with EtOAc, washed three times with saturated $NaHCO_3$ solution and once with brine, dried, and evaporated. The resulting crude is purified by column chromatography on silica gel with CH_2Cl_2/CH_3OH (95:5) to give a tan solid (144 mg, 22%, diastereomeric ratio: 1:1). $C_{38}H_{49}N_5O_5$ MW: 655.83 g/mol. HRMS (ESI-TOF) *m/z* $[M + H]^+$: (calcd) 656.3812; (found) 656.3829. HPLC−MS t_R: 10.32 min. *m/z* $[M + H]^+$: 656.2. ^{1}H NMR ($CDCl_3$, 600 MHz): δ = 0.08 (1.5H, d, J = 7), 0.72−0.84 (2H, m), 0.87 (1.5 H, d, J = 7), 0.97−1.08 (1H, m), 1.12−1.53 (12H, m), 2.25−2.37 (0.5H, m), 2.70−2.84 (0.5H, m), 2.98−3.09 (0.5H, m), 3.29−3.46 (1H, m), 3.46−3.58 (1H, m), 3.58−3.72 (1H, m), 3.72−3.85 (1H, m), 3.85−3.92 (0.5H, m), 3.92−4.05 (1H, m), 4.05−4.18 (0.5H, m), 4.18−4.30 (0.5H, m), 14.18−4.45 (1.5H, m), 4.45−4.59 (0.5H, m), 4.59−4.81 (1.5H, m), 4.814.93 (0.5H, m), 5.79 (0.5H, s), 5.97(0.5H, s), 6.02 (0.5H, d, J = 10), 6.08 (0.5H, d, J = 11), 6.96−7.50 (15H, m), 9.25 (0.5H, s), 9.71 (0.5H, s), 9.79 (0.5H, s), 10.05 (0.5H, s). ^{13}C NMR ($CDCl_3$, 600 MHz): δ = 18.2, 18.7, 19.4, 20.6, 28.3, 28.6, 44.7, 48.2, 49.3, 51.1, 52.4, 52.5, 57.4, 59.7, 80.4, 127.1, 127.5, 128.6, 129.4, 140.8, 142.2, 155.9, 167.1, 175.6.

1-((*S*)-2-((*S*)-2-Aminopropanamido)-3-methylbutanoyl)-*N*-benzhydryl-4-benzylpiperazine-2-carboxamide (15). In a 5 mL round-bottom flask is placed *tert*-butyl 1-(1-(2-(benzhydrylcarbamoyl)-4-benzylpiperazin-1-yl)-3-methyl-1-oxobutan-2-ylamino)-1-oxopropan-2-ylcarbamate **13** (0.05 mmol, 33 mg), and trifluoroacetic acid is added (100 μL). The solution is stirred for 10 min, and the trifluoroacetic acid residue is evaporated. A TLC plate DCM/MeOH 9:1 + 1% Et_3N on the crude gives a yellow solid **15** (15.5 mg, 56%). $C_{33}H_{41}N_5O_3$, MW: 555.71 g/mol. HRMS (ESI-TOF) *m/z* $[M + H]^+$: (calcd) 556.3288; (found) 556.3251. HPLC−MS t_R: 8.71 min. *m/z* $[M + H]^+$: 556.1.

***tert*-Butyl 1-(1-(7-(Benzhydrylcarbamoyl)-4-cyclohexyl-1,4-diazepan-1-yl)-3-methyl-1-oxobutan-2-yl amino)-1-oxopropan-2-ylcarbamate (17).** To a solution of *N*-(3-aminopropyl)cyclohexylamine **16** (2 mmol, 340 μL) and BocAlaValOH **6** (2.12 mmol, 611 mg) in 2 mL of MeOH is added diphenyl isocyanide **7** (425 mg, 2.2 mmol) and aqueous chloroacetaldehyde solution **1** (4 mmol, 50% wt sol., 516 μL). The reaction mixture is stirred at room temperature for 5 days. The reaction mixture is diluted with EtOAc, washed three times with saturated $NaHCO_3$ solution and once with brine, dried, and evaporated. The resulting crude is purified by column chromatography on silica gel with EtOAc/MeOH 8:2 to give a tan solid **17** (99 mg, 7%, diastereomeric ratio: 4/6). $C_{38}H_{55}N_5O_5$, MW: 661.87 g/mol. HRMS (ESI-TOF) *m/z* $[M + H]^+$: (calcd) 661.420320; (found) 661.421219. HPLC−MS t_R: 9.97 min. *m/z* $[M + H_2O]^+$: 680.3. ^{1}H NMR ($CDCl_3$, 600 MHz): δ = 0.50−0.97 (8H, m), 0.97−1.19 (5H, m), 1.19−1.28 (3H, m), 1.32 (4.5H, s), 1.33 (4.5H, s), 1.38−1.49 (2H, m), 1.49−1.62 (1H, m), 1.62−1.79 (2H, m), 1.78−2.18 (4H, m), 2.67−3.00 (3H, m), 3.87−4.61 (4H, m), 5.19 (0.5H, s), 5.35 (0.5H, s), 6.16 (0.5H, d, J = 8), 6.20 (0.5H, d, J = 8), 7.10−7.30 (11H, m), 8.38 (0.5H, s), 8.48 (0.5H, s). ^{13}C NMR ($CDCl_3$, 600 MHz): δ = 17.8, 18.2, 19.1, 24.5, 24.8, 28.3, 29.0, 30.6, 43.2, 45.2, 50.0, 57.1, 57.6, 58.4, 64.3, 79.9, 127.4, 127.8, 128.6, 128.7, 141.4, 155.6, 171.2, 173.2.

1-((*S*)-2-((*S*)-2-Aminopropanamido)-3-methylbutanoyl)-*N*-benzhydryl-4-cyclohexyl-1,4-diazepane-2-carboxamide 2,2,2-Trifluoroacetate (18). In a 5 mL round-bottom flask is placed *tert*-butyl 1-(1-(7-(benzhydrylcarbamoyl)-4-cyclohexyl-1,4-diazepan-1-yl)-3-methyl-1-oxobutan-2-ylamino)-1-oxopropan-2-ylcarbamate **17** (0.07 mmol, 47 mg), and trifluoroacetic acid is added (100 μL). The solution is stirred for 10 min and the trifluoroacetic acid residue is evaporated to give a tan solid (58 mg, quantitative yield). $C_{35}H_{48}F_3N_5O_5$, MW: 675.78 g/mol. HRMS (ESI-TOF) *m/z* $[M + H_2O]^+$: (calcd) 580.3863; (found) 580.3815. HPLC−MS t_R: 8.15 min. *m/z* $[M + H_2O]^+$: 580.0.

BocAlaSH (20). To a solution of BocAlaOH **19** (5 g, 26 mmol) in DMF (26 mL) is added carbonyldiimidazole (8.6 g, 53 mmol), and the reaction mixture is stirred at room temperature for 4 h. NaSH (5.8 g, 104 mmol) is then added, and stirring continued at room temperature for 16 h. The reaction mixture is poured in HCl, 2 N, and extracted with AcOEt. The organic layer is then washed with brine, dried over Na_2SO_4, and evaporated. A white solid **20** was obtained (5 g, 94%). $C_8H_{15}NO_3S$, MW: 205.27 g/mol. ^{1}H NMR ($CDCl_3$, 600 MHz): δ = 1.44 (3H, d, J = 7), 1.46 (9H, s), 4.30 (0.4H, s), 4.52 (0.6H, s), 5.31 (0.7H, s), 5.48 (0.3H). ^{13}C NMR ($CDCl_3$, 600 MHz): δ = 18.07, 28.07, 57.22, 80.79, 154.94, 196.83.

Methyl 2-(1-((*S*)-2-(*tert*-Butoxycarbonylamino)-*N*-(2,4-dimethoxybenzyl)propanamido)-2-methylpropyl)thiazole-4-carboxylate (24). The isobutyraldehyde **21** (91 μL, 1 mmol) is added under nitrogen at 0 °C to a solution of 2,4 dimethoxybenzylamine **22** (152 μL, 1 mmol) in MeOH (0.5 mL) and treated with $MgSO_4$ (120 mg, 1 mmol). The Schiff base is precondensed for 1 h, and the solution is cooled to −10 °C. Then BocAlaSH **20** (205 mg, 1 mmol) and the methyl 3-(dimethylamino)-2-isocyanoacrylate **23** (154 mg, 1 mmol) are added and the reaction volume is increased to 1 mL. The reaction mixture is allowed to warm to room temperature and stirred for 3 days. The solvent is removed in vacuo, and the residue is treated with dichloromethane and water. The organic layer is separated and washed several times with HCl (3%) and with saturated $NaHCO_3$ solution, dried over Na_2SO_4, and concentrated in vacuo. The resulting crude is purified by silica gel column chromatography. The eluting mixture petroleum ether/ethyl acetate 8:2 affords separation between the two diastereomers **24** to give a white solid (125 mg, 23%, diastereomeric ratio: 1:1). $C_{26}H_{37}N_3O_7S$, MW: 535.65 g/mol. ^{1}H NMR ($CDCl_3$, 600 MHz): δ = 0.70 (1H, s), 0.77 (3H, d, J = 7), 0.92 (2H, d, J = 7), 1.23−1.35 (3H, m), 1.44 (4.5H, s), 1.45 (4.5H, s), 2.91−3.04 (1H, m), 3.64 (2H, s), 3.76 (3H, s), 3.78 (1H, s), 3.89 (2H, s), 3.92 (1H, s), 4.36−4.50 (1H, m), 4.58−4.76 (2H, m), 4.86−4.98 (1H, m), 5.42−5.48 (0.5H, m), 5.54−5.60 (0.5H, m), 6.20 (1H, s), 6.29−6.39 (2H, m), 6.89−6.98 (1H, m), 8.03 (0.5H, s), 8.05 (0.5H, s). ^{13}C NMR ($CDCl_3$, 600 MHz): δ = 19.01, 19.54, 20.41, 20.57, 28.35, 29.70, 30.33, 47.21, 52.23, 54.90, 55.24, 79.38, 98.11, 101.98, 103.57, 116.30, 129.05, 130.39, 144.82, 154.99, 158.40, 168.87, 161.82, 169.21, 174.16.

***tert*-Butyl (2*S*)-1-((1-(4-(Benzylcarbamoyl)thiazol-2-yl)-2-methylpropyl)-(2,4-dimethoxybenzyl)amino)-1-oxopropan-2-ylcarbamate (26).** To a stirred solution of methyl 2-(1-((*S*)-2-(*tert*-butoxycarbonylamino)-*N*-(2,4-dimethoxybenzyl) propanamido)-2-methylpropyl)thiazole-4-carboxylate **24** (54 mg, 0.1 mmol) is added TBD (4 mg, 0.03 mmol) followed by benzylamine **25** (13 μL, 0.12 mmol) under nitrogen atmosphere. The reaction mixture is slowly warmed to 75 °C and stirred for 12 h, allowed to cool to room temperature, and concentrated in vacuo. The residue obtained is chromatographed on silica gel using petroleum ether/ethyl acetate 6:4 as eluent to afford a white solid **25** (43.6 mg, 71%). $C_{32}H_{42}N_4O_6S$, MW: 610.76 g/mol. HRMS (ESI-TOF) m/z $[M + Na]^+$: (calcd) 633.2723; (found) 633.2722. ^{1}H NMR ($CDCl_3$, 600 MHz): δ = 0.79 (3H, d, J = 7), 0.83 (1H, s), 0.94 (2H, d, J = 7), 1.21−1.31 (3H, m), 1.41 (4.5H, s), 1.43 (4.5H, s), 2.75−2.89 (1H, m), 3.56 (1.5H, s), 3.58 (1.5H, s), 3.69 (1.5H, s), 3.70 (1.5H, s), 4.44−4.80 (6H, m), 5.32−5.39 (0.5H, m), 5.50−5.55 (0.5H, m), 6.15−6.26 (3H, m), 6.62 (1H, s), 7.21−7.40 (5H, m), 7.94 (0.5H, s), 7.96 (0.5H, s). ^{13}C NMR ($CDCl_3$, 600 MHz): δ = 19.25, 19.32, 20.60, 21.06, 28.33, 30.13, 43.16, 46.86, 47.41, 53.43, 54.93, 79.40, 97.97, 98.34, 103.68, 116.21, 116.67, 124.25, 127.45, 127.78, 128.70, 138.34, 154.74, 155.05, 160.67, 161.03, 161.10, 168.22, 174.20.

2-(1-((*S*)-2-Aminopropanamido)-2-methylpropyl)-*N*-benzylthiazole-4-carboxamide (27). To the *tert*-butyl (2*S*)-1-((1-(4-(benzylcarbamoyl)thiazol-2-yl)-2-methylpropyl)-(2,4-dimethoxybenzyl)amino)-1-oxopropan-2-ylcarbamate **26** (44 mg, 0.07 mmol) is added TFA (700 μL), and the mixture is refluxed overnight. TFA is removed in vacuo and the crude residue is purified by silica gel column chromatography with a gradient eluting mixture ethyl acetate/methanol and subsequently by TLC plate with the same mixture to give a white solid **27** (5 mg, 20%). $C_{18}H_{24}N_4O_2S$, MW: 360.47 g/mol. HRMS (ESI-TOF) m/z $[M + H]^+$: (calcd) 361.1698; (found) 361.1688. HPLC−MS t_R: 8.43 min. m/z $[M + H]^+$: 360.9. ^{1} H NMR ($CDCl_3$, 600 MHz): δ = 0.93−1.02 (6H, m), 1.35−1.44 (3H, m), 1.87 (2H, s), 2.36−2.46 (1H, m), 3.58−3.68 (1H, m), 4.62−4.72 (2H, m), 5.11−5.18 (1H, m), 7.27−7.34 (2H, m), 7.34−7.43 (3H, m), 7.66 (1H, s), 8.04−8.12 (2H, m).

Methyl 2-(1-((*S*)-2-(*tert*-Butoxycarbonylamino)-*N*-(2,4-dimethoxybenzyl)propanamido)-2-methylpropyl)-5-phenylthiazole-4-carboxylate (32). The isobutyraldehyde **21** (183 μL, 2 mmol), the 2,4 dimethoxybenzylamine **22** (304 μL, 2 mmol), and $MgSO_4$ (241 mg, 2 mmol) are stirred under inert and water-free conditions in dry MeOH (2 mL) at 0 °C. The imine is precondensed for 2 h, and the solution is cooled to −10 °C. BocAlaSH **20** (411 mg, 2 mmol) and (*Z*)-methyl 3-bromo-2-isocyano-3-phenylacrylate **31** (532 mg, 2 mmol) are added, and the reaction volume is increased to 4 mL. The mixture is allowed to warm to room temperature and stirred for 48 h. Then the reaction mixture is diluted with dichloromethane and the organic layer is washed with saturated $NaHCO_3$ solution, 3% HCl, and saturated NaCl solution, dried over $NaSO_4$, and concentrated in vacuo. The resulting compound **32** could not be efficiently purified by silica gel chromatography, so the crude compound was used directly for the following reaction. $C_{32}H_41N_3O_7S$, MW: 611.75 g/mol.

***tert*-Butyl (2*S*)-1-((1-(4-(Benzylcarbamoyl)-5-phenylthiazol-2-yl)-2-methylpropyl)-(2,4-dimethoxybenzyl)amino)-1-oxopropan-2-ylcarbamate (33).** To a stirred solution of the methyl 2-(1-((*S*)-2-(*tert*-butoxycarbonylamino)-*N*-(2,4-dimethoxybenzyl)propanamido)-2-methylpropyl)-5-phenylthiazole-4-carboxylate **32** (crude mixture: 396 mg, 0.65 mmol) is added TBD (27 mg, 0.195 mmol) followed by benzylamine **25** (85 μL, 0.78 mmol) under nitrogen atmosphere. The reaction mixture is slowly warmed to 75 °C and stirred for 12 h, allowed to cool to room temperature, and concentrated in vacuo. The residue obtained is chromatographed on silica gel using petroleum ether/ethyl acetate as eluent to afford a yellow solid **33** (20 mg). $C_{38}H_{46}N_4O_6S$, MW: 686.86 g/mol. ^{1}H NMR ($CDCl_3$, 600 MHz): δ = 0.69−1.13 (6H, m), 1.20−1.38 (3H, m), 1.38−1.50 (9H, m), 2.79−2.93 (0.5H, m), 2.93−3.05 (0.5H, m), 3.49 (1H, s), 3.59 (1H, s), 3.65−3.89 (4H, m), 4.41−4.99 (6H, m), 5.33−5.42 (0.5H, m), 5.55−5.63 (0.5H, m), 6.21−6.31 (1H, m), 6.31−6.40 (1H, m), 6.40−6.53 (1H, m), 6.65−6.84 (0.5 H, m), 6.89−7.06 (0.5 H, m), 7.20−7.59 (10H, m). ^{13}C NMR ($CDCl_3$, 600 MHz): δ = 19.04, 19.31, 19.59, 20.62, 28.33, 29.71, 30.15, 43.00, 43.79, 46.87, 47.47, 50.85, 55.00, 55.28, 79.37, 98.27, 103.39, 116.03, 127.34, 127.70, 127.88, 127.90, 127.93, 128.07, 128.61, 128.64, 128.99, 129.74, 130.17, 138.58, 154.86, 158.50, 159.64, 160.78, 161.46, 162.60, 165.22, 173.76, 174.22.

2-(1-((*S*)-2-Aminopropanamido)-2-methylpropyl)-*N*-benzyl-5-phenylthiazole-4-carboxamide (34). To the *tert*-butyl (2*S*)-1-((1-(4-(benzylcarbamoyl)-5-phenylthiazol-2-yl)-2-methylpropyl)-(2,4-dimethoxybenzyl)amino)-1-oxopropan-2-ylcarbamate **33** (20 mg, 0.03 mmol) is added TFA (200 μL), and the mixture is refluxed overnight. TFA is removed in vacuo and the crude residue is purified by silica gel column chromatography with the eluting mixture ethyl acetate/methanol 9:1 to give a yellow solid **34** (6 mg, 46%). $C_{24}H_{28}N_4O_2S$, MW: 436.57 g/mol. HRMS (ESI-TOF) m/z $[M + H]^+$: (calcd) 437.2011; (found) 437.2007. HPLC−MS t_R: 10.85. m/z $[M + H]^+$: 437.0. ^{1} H NMR ($CDCl_3$, 600 MHz): δ = 0.76−1.08 (6H, m), 1.31−1.58 (3H, m), 2.24−2.40 (1H, m), 3.56−3.71 (1H, m), 4.29−4.55 (2H, m), 4.87−5.05 (1H, m), 7.03−7.59 (10H, m), 8.17−8.56 (2H, m), 8.71−8.82 (1H, m), 8.92−9.03 (1H, m) . ^{13} C NMR ($CDCl_3$, 600 MHz): δ = 17.42, 17.90, 18.43, 19.34, 29.72, 33.14, 43.30, 49.45, 52.16, 55.39, 56.77, 127.38, 128.18, 128.25, 128.60, 128.74, 128.81, 129.00, 129.36, 129.86, 130.02, 139.35, 147.06, 162.99, 168.44, 169.63, 170.63.

***tert*-Butyl (2*S*)-1-((2*S*)-1-Hydroxy-3-methyl-1-(1-phenethyl-1*H*-tetrazol-5-yl)butan-2-ylamino)-1-oxopropan-2-ylcarbamate (38).** To a solution of BocAlaValH **35** (170 mg, 0.6 mmol) and phenethyl isocyanide **36** (79 mg, 0.6 mmol) in 1 mL of dichloromethane is added $TMSN_3$ **37** (69 mg, 0.6 mmol), and the reaction mixture is stirred at room temperature for 4 days. The solution is concentrated and the crude residue is purified by silica gel column chromatography with the eluting mixture dichloromethane/methanol 95:5 and subsequently by TLC plate with the same mixture to give a white foam **38** (55 mg, 20%). $C_{22}H_{34}N_6O_4$, MW: 446.54 g/mol. HRMS (ESI-TOF) m/z $[M + Na]^+$: (calcd) 469.2539; (found) 469.2560. HPLC−MS t_R: 10.46. m/z $[M + H]^+$: 447.1. ^{1} H NMR ($CDCl_3$, 600 MHz): δ = 0.55−1.03 (6H, m), 1.03−1.22 (3H, m), 1.22−1.63 (9H, m), 1.82−2.31 (1H, m), 3.14−3.38 (2H, m), 3.53−3.83 (1H, m), 3.88−4.28 (1H, m), 4.45−4.90 (3H, m), 5.08−5.44 (1H, m), 7.04−7.19(2H, m), 7.19−7.38 (3H, m). ^{13} C NMR ($CDCl_3$, 600 MHz): δ = 18.16, 19.04, 19.48, 19.92, 27.64, 28.25, 35.96, 36.34, 39.22, 49.71, 50.64, 51.99, 58.93, 60.63, 62.40, 66.13, 80.15, 80.81, 127.32, 128.84, 136.73, 155.54, 174.29.

(2*S*)-2-Amino-*N*-((2*S*)-1-hydroxy-3-methyl-1-(1-phenethyl-1*H*-tetrazol-5-yl)butan-2-yl)propanamide (39). In a 5 mL round-bottom flask is placed *tert*-butyl (2*S*)-1-((2*S*)-1-hydroxy-3-methyl-1-(1-phenethyl-1*H*-tetrazol-5-yl)butan-2-ylamino)-1-oxopropan-2-ylcarbamate **38** (0.06 mmol, 28 mg), and trifluoroacetic acid is added (100 μL). The solution is stirred for 1 h, and the trifluoroacetic acid residue is evaporated. A silica gel column chromatography with a gradient eluting mixture DCM/MeOH on the crude gives a colorless solid **39** (10 mg, 50%). $C_{17}H_{26}N_6O_2$, MW: 346.43 g/mol. HRMS (ESI-TOF) m/z $[M + H]^+$: (calcd) 347.2195; (found) 347.2193. HPLC−MS t_R: 8.20. m/z $[M + H]^+$: 347.0. ^{1} H NMR ($CDCl_3$, 600 MHz): δ = 0.53−1.15 (4H, m), 1.15−1.40 (1H, m), 1.40−1.79 (4H, m), 1.79−1.93 (0.5H, m), 1.93−2.11 (0.5H, m), 3.06−3.42 (2H, m), 3.81−4.39 (2H, m), 4.49−5.02 (2H, m), 5.19−5.35 (0.5H, m), 5.35−5.51 (0.5H, m), 6.94−7.17 (2H, m), 7.17−7.36 (3H, m), 8.33 (0.3H,s), 8.42 (0.4H, s), 8.56 (0.3H, s).

Biology. NMR Spectroscopy. Spectra were acquired on a 600 MHz Bruker Avance spectrometer equipped with TXI probe and z-shielded gradient coils or on a 600 MHz Bruker Avance equipped with TCI cryoprobe. Dissociation equilibrium

constants (K_d) of ligands were determined by monitoring the protein chemical shift changes as a function of ligand concentration. Data were collected for a set of resolved BIR3 (concentration was 100 μM) ^{1}H NMR resonances and fitted to a single binding site model according to the following equation:[52]

$$K_d = [T_o](1-p)([L_o]-[T_o]p)/([T_o]p)$$

$[T_o]$ and $[L_o]$ are total concentration of target protein and ligand, respectively. The parameter p represents the fractional population of bound versus free species at equilibrium, which for fast exchanging ligands is measured as

$$p = (\delta_{obs}-\delta_f)/(\delta_{sat.}-\delta_{free})$$

δ_{obs} is the observed receptor chemical shift during the titration, and δ_{free} and $\delta_{sat.}$ are the chemical shifts for the receptor in the unbound and fully bound (saturated) states, respectively. Compounds with estimated K_d values of 100 μM or less are subsequently determined more accurately by a more complete NMR titration. At least six data points were collected for different concentrations of ligand, and K_d can then be determined by a nonlinear least-squares fit of p versus $[L_o]$.

$$p = \{([T_o]+[L_o]+K_d) - \sqrt{(([T_o]+[L_o]+K_d)^2-4[L_o][T_o])}\}/(2[T_o])$$

All NMR data were processed and analyzed using TOPSPIN2.0 (Bruker BioSpin Corp., Billerica, MA) and SPARKY.[53] For chemical shift mapping the NMR samples contained 0.1 mM ^{15}N-labeled BIR3, 100 mM potassium phosphate buffer (pH 7.0), 5% DMSO, and 7% D_2O. 2D [^{15}N, ^{1}H]HSQC experiments were acquired using 32 scans with 2048 and 128 complex data points in the ^{1}H and ^{15}N dimensions at 300 K.

Isothermal Titration Calorimetry (ITC). Purified BIR3 domain of XIAP and the compounds were dissolved in PBS buffer (pH 7.4) and then degassed for 10 min prior to sample loading. Titrations were performed using a VP-ITC calorimeter from Microcal (Northampton, MA). The solution containing BIR3 (100 μM) was loaded into the sample cell, whereas the compounds' solution (1 mM) was loaded into the injection syringe. The calorimeter was first equilibrated at 25 °C, and the baseline was monitored during equilibration. The total observed heat effects were corrected for these small contributions. All titration data were analyzed using Microcal Origin software provided by the ITC manufacturer (MicroCal, LLC.). The association constant (K_a) is obtained through the equation $\Delta G = -RT\ln K_a$, where R is the gas constant and T is the absolute temperature in kelvin. Equilibrium dissociation constant (K_d) was calculated as the reciprocal of K_a.

Time-Resolved Fluorescence Resonance Energy Transfer (TR-FRET) Assay.[54] To each well of 96-well black plates (PerkinElmer), 25 μL of detection buffer (Perkin-Elmer), 5 μL of a variable concentration of biotin-labeled SMAC N-terminal peptide (Biotin-lc-G-G-I-P-V-A) 10 nM was added together with 5 μL of a solution containing the 10 nM BIR3 protein and 5 μL in DMSO solution containing the test compounds in various concentrations. After incubation for 1 h at 4 °C, to each well is added a 5 μL solution of 5 nM Eu−antibody conjugate and 5 μL of solution containing 2 nM APC−streptavidin. The plates were incubated at 4 °C overnight, and the measurements were taken by Wallac 1420 plate reader (PerkinElmer). The excitation wavelength is 340 nm, and the emission wavelength is 665 nm. The same concentrations of DMSO solutions were used to replace the amount of compounds' solutions as positive controls. The solutions without SMAC peptide and BIR3 protein (the volumes were replaced by the buffer) were used as native controls. Z factor measurements were obtained by repeating the experiments (positive and negative controls) multiple times. The assay was performed by two independent experiments and each having two wells per drug concentration.

Cell Culture and ATPlite Cell Viability Assay. ER-negative MDA-MB 231 breast cancer cells were obtained from the American Type Culture Collection (Manassas, VA) and were maintained in DMEM medium supplemented with 10% fetal bovine serum (FBS, Gibco) at 37 °C in a humidified incubator containing 5% CO_2. The effect of individual test agents on cell viability was assessed by using the ATPlite one step luminescence assay system (PerkinElmer, Waltham, MA)[55] in four replicates. For cell viability data of compounds and AVPI, MDA-MB-231, cells (5000 cells/well) were seeded and incubated in white 96-well, flat-bottomed plates in DMEM medium with 10% FBS overnight. The cells were exposed to various concentrations of test agents dissolved in DMSO (final DMSO concentration, 0.1%) in serum free DMEM medium for 72 h. After the indicated length of treatments, the cells in each well were treated with 10 μL ATPlite substrate solution. The plate was dark-adapted for 5−10 min, and the luminescence was measured by a Wallac 1420 plate reader (PerkinElmer). The curves or graphs were generated using Excel (Microsoft), and the IC_{50} was calculated by PRISM (Graphpad).

References

(1) Yip, K. W.; Reed, J. C. Bcl-2 family proteins and cancer. *Oncogene* **2008**, *27*, 6398–6406.

(2) Fulda, S. Inhibitor of apoptosis (IAP) proteins: novel insights into the cancer-relevant targets for cell death induction. *ACS Chem. Biol.* **2009**, *4*, 499–501.

(3) Sun, H.; Nikolovska-Coleska, Z.; Yang, C. Y.; Qian, D.; Lu, J.; Qiu, S.; Bai, L.; Peng, Y.; Cai, Q.; Wang, S. Design of small-molecule peptidic and nonpeptidic Smac mimetics. *Acc. Chem. Res.* **2008**, *41*, 1264–1277.

(4) Schimmer, A. D.; Welsh, K.; Pinilla, C.; Wang, Z.; Krajewska, M.; Bonneau, M. J.; Pedersen, I. M.; Kitada, S.; Scott, F. L.; Bailly-Maitre, B.; Glinsky, G.; Scudiero, D.; Sausville, E.; Salvesen, G.; Nefzi, A.; Ostresh, J. M.; Houghten, R. A.; Reed, J. C. Small-molecule antagonists of apoptosis suppressor XIAP exhibit broad antitumor activity. *Cancer Cell* **2004**, *5*, 25–35.

(5) Huang, Y.; Rich, R. L.; Myszka, D. G.; Wu, H. Requirement of both the second and third BIR domains for the relief of X-linked inhibitor of apoptosis protein (XIAP)-mediated caspase inhibition by Smac. *J. Biol. Chem.* **2003**, *278*, 49517–49522.

(6) Gao, Z.; Tian, Y.; Wang, J.; Yin, Q.; Wu, H.; Li, Y. M.; Jiang, X. A dimeric Smac/Diablo peptide directly relieves caspase-3 inhibition by XIAP: dynamic and cooperative regulation of XIAP by SMAC/DIABLO. *J. Biol. Chem.* **2007**, *282*, 30718–30727.

(7) Park, C. M.; Sun, C.; Olejniczak, E. T.; Wilson, A. E.; Meadows, R. P.; Betz, S. F.; Elmore, S. W.; Fesik, S. W. Non-peptidic small molecule inhibitors of XIAP. *Bioorg. Med. Chem. Lett.* **2005**, *15*, 771–775.

(8) Sun, H.; Nikolovska-Coleska, Z.; Chen, J.; Yang, C. Y.; Tomita, Y.; Pan, H.; Yoshioka, Y.; Krajewski, K.; Roller, P. P.; Wang, S. Structure-based design, synthesis and biochemical testing of novel and potent Smac peptido-mimetics. *Bioorg. Med. Chem. Lett.* **2005**, *15*, 793–797.

(9) Sun, H.; Nikolovska-Coleska, Z.; Lu, J.; Meagher, J. L.; Yang, C. Y.; Qiu, S.; Tomita, Y.; Ueda, Y.; Jiang, S.; Krajewski, K.; Roller, P. P.; Stuckey, J. A.; Wang, S. Design, synthesis, and characterization of a potent, nonpeptide, cell-permeable, bivalent Smac mimetic that concurrently targets both the BIR2 and BIR3 domains in XIAP. *J. Am. Chem. Soc.* **2007**, *129*, 15279–15294.

(10) Wist, A. D.; Gu, L.; Riedl, S. J.; Shi, Y.; McLendon, G. L. Structure−activity based study of the Smac-binding pocket within the BIR3 domain of XIAP. *Bioorg. Med. Chem.* **2007**, *15*, 2935–2943.

(11) Oost, T. K.; Sun, C.; Armstrong, R. C.; Al-Assaad, A. S.; Betz, S. F.; Deckwerth, T. L.; Ding, H.; Elmore, S. W.; Meadows, R. P.; Olejniczak, E. T.; Oleksijew, A.; Oltersdorf, T.; Rosenberg, S. H.; Shoemaker, A. R.; Tomaselli, K. J.; Zou, H.; Fesik, S. W. Discovery of potent antagonists of the antiapoptotic protein XIAP for the treatment of cancer. *J. Med. Chem.* **2004**, *47*, 4417–4426.

(12) Vucic, D.; Franklin, M. C.; Wallweber, H. J. A.; Das, K.; Eckelman, B. P.; Shin, H.; Elliott, L. O.; Kadkhodayan, S.; Deshayes, K.; Salvesen, G. S.; Fairbrother, W. J. Engineering ML-IAP to produce an extraordinarily potent caspase 9 inhibitor: implications for Smac-dependent anti-apoptotic activity of ML-IAP. *Biochem. J.* **2005**, *385*, 11–20.

(13) Zobel, K.; Wang, L.; Varfolomeev, E.; Franklin, M. C.; Elliott, L. O.; Wallweber, H. J. A.; Okawa, D. C.; Flygare, J. A.; Vucic, D.; Fairbrother, W. J.; Deshayes, K. Design, synthesis, and biological activity of a potent Smac mimetic that sensitizes cancer cells to apoptosis by antagonizing IAPs. *ACS Chem. Biol.* **2006**, *1*, 525–533.

(14) Gaither, A.; Porter, D.; Yao, Y.; Borawski, J.; Yang, G.; Donovan, J.; Sage, D.; Slisz, J.; Tran, M.; Straub, C.; Ramsey, T.; Iourgenko, V.; Huang, A.; Chen, Y.; Schlegel, R.; Labow, M.; Fawell, S.; Sellers, W. R.; Zawel, L. A Smac mimetic rescue screen reveals roles for inhibitor of apoptosis proteins in tumor necrosis factor-α signaling. *Cancer Res.* **2007**, *67*, 11493–11498.

(15) Huang, J. W.; Zhang, Z.; Wu, B.; Cellitti, J. F.; Zhang, X.; Dahl, R.; Shiau, C. W.; Welsh, K.; Emdadi, A.; Stebbins, J. L.; Reed, J. C.; Pellecchia, M. Fragment-based design of small molecule X-linked inhibitor of apoptosis protein inhibitors. *J. Med. Chem.* **2008**, *51*, 7111–7118.

(16) Chauhan, P. D.; Neri, P.; Velankar, M.; Podar, K.; Hideshima, T.; Fulciniti, M.; Tassone, P.; Raje, N.; Mitsiades, C.; Mitsiades, N.; Richardson, P.; Zawel, L.; Tran, M.; Munshi, N.; Anderson, K. C. Targeting mitochondrial factor Smac/DIABLO as therapy for multiple myeloma (MM). *Blood* **2007**, *109*, 1220–1227.

(17) Sun, W.; Nikolovska-Coleska, Z.; Qin, D.; Sun, H.; Yang, C. Y.; Bai, L.; Qiu, S.; Wang, Y.; Ma, D.; Wang, S. Design, synthesis, and evaluation of a potent, cell-permeable, conformationally constrained second mitochondria derived activator of caspase (Smac) mimetic. *J. Med. Chem.* **2009**, *52*, 593–596.

(18) Czarna, A.; Beck, B.; Srivastava, S.; Popowicz, G. M.; Wolf, S.; Huang, Y.; Bista, M.; Holak, T. A.; Dömling, A. Robust generation of lead compounds for protein−protein interactions by computational and MCR chemistry: p53/Hdm2 antagonists. *Angew. Chem., Int. Ed.* **2010**, *49*, 5352–5356.

(19) Popowicz, G. M.; Czarna, A.; Wolf, S.; Wang, K.; Wang, W.; Dömling, A.; Holak, T. A. Structures of low molecular weight inhibitors bound to MDMX and MDM2 reveal new approaches for p53-MDMX/MDM2 antagonist drug discovery. *Cell Cycle* **2010**, *9*, 1104–1111.

(20) Bista, M.; Kowalska, K.; Janczyk, W.; Dömling, A.; Holak, T. Monitoring the effects of antagonists on protein−protein interactions with NMR spectroscopy. *J. Am. Chem. Soc.* **2009**, *131*, 7500–7501.

(21) Dömling, A. Recent developments in isocyanide based multicomponent reactions in applied chemistry. *Chem. Rev.* **2006**, *106*, 17–89.

(22) Pirok, G.; Mate, N.; Varga, J.; Szegezdi, J.; Vargyas, M.; Dorant, S.; Csizmadia, F. Making "real" molecules in virtual space. *J. Chem. Inf. Model.* **2006**, *46*, 563–568.

(23) Gerber, P. R.; Müller, K. MAB, a generally applicable molecular force field for structure modeling in medicinal chemistry. *J. Comput.-Aided Mol. Des.* **1995**, *9*, 251–268.

(24) Dömling, A.; Ugi, I. The seven-component reaction. *Angew. Chem., Int. Ed. Engl.* **1993**, *32*, 563–564.

(25) Rossen, K.; Pye, P. J.; DiMichele, L. M.; Volante, R. P.; Reider, P. J. An efficient asymmetric hydrogenation approach to the synthesis of the Crixivan piperazine intermediate. *Tetrahedron Lett.* **1998**, *39*, 6823–6826.

(26) Rossen, K.; Weissman, S. A.; Sager, J.; Reamer, R. A.; Askin, D.; Volante, R. P.; Reider, P. J. Asymmetric hydrogenation of tetrahydropyrazines: synthesis of (*S*)-piperazine-2-*tert*-butylcarboxamide, an intermediate in the preparation of the HIV protease inhibitor indinavir. *Tetrahedron Lett.* **1995**, *36*, 6419–6422.

(27) Heck, S.; Dömling, A. A versatile multi-component one-pot thiazole synthesis. *Synlett* **2000**, 424–426.

(28) Nixey, T.; Hulme, C. Rapid generation of cis-constrained norstatine analogs using a $TMSN_3$-modified Passerini MCC/N-capping strategy. *Tetrahedron Lett.* **2002**, *43*, 6833–6835.

(29) Gröger, H.; Martens, J.; Goerlich, J. R.; Schmutzler, R. A novel synthetic approach to α-aminophosphine sulfide structures: the first addition of dimethylephosphine sulfide to 3-thiazolines. *Phosphorus, Sulfur Silicon Relat. Elem.* **1997**, *128*, 153–163.

(30) Thiel, M.; Asinger, F.; Schmiedel, K. Uber die gemeinsame einwirkung von elementarem schwefel und gasförmigem ammoniak auf ketone VIII. Die kondensation von α-mercaptoaldehyden mit oxo-verbindungen und gasförmigem ammoniak zu thiazolinen-Δ. *Justus Liebigs Ann. Chem.* **1958**, *611*, 121–131.

(31) Martens, J.; Offermanns, H.; Scherberich, P. Facile synthesis of racemic cysteine. *Angew. Chem., Int. Ed. Engl.* **1981**, *20*, 668.

(32) Dömling, A.; Ugi, I. A new 5,6-dihydro-2*H*-1,3-oxazine synthesis via Asinger-type condensation. *Tetrahedron* **1993**, *49*, 9495–9500.

(33) Hatam, M.; Tehranfar, D.; Martens, J. A novel and convenient route to phosphono oligopeptides derived from 1,3-oxazolines, 1, 3-oxazines and 1,3-thiazolines. *Synth. Commun.* **1995**, *25*, 1677–1688.

(34) Gröger, H.; Hatam, M.; Martens, J. Synthese totalgeschützter, nichtproteinogener α-aminosäuren und oligopeptide aus 2*H*-1,3-oxazinen und 2*H*-1,3-benzoxazinen via Ugi-reaktion. *Tetrahedron* **1995**, *51*, 7173–7180.

(35) Hatam, M.; Martens, J. Phosphinic acid analogues of thiaproline and the related heterocyclic amino acids. *Synth. Commun.* **1995**, *25*, 2553–2559.

(36) Hatam, M.; Goerlich, J. R.; Schmutzler, R.; Gröger, H.; Martens, J. The totally protected hydroxy containing α-amino phosphinic esters and α-amino phosphinoxides as well as their carbamoyl derivatives. *Synth. Commun.* **1996**, *26*, 3685–3698.

(37) Dömling, A.; Illgen, K. 1-Isocyano-2-dimethylamino-alkenes: versatile reagents in diversity-oriented organic synthesis. *Synthesis* **2005**, 662–667.

(38) Henkel, B.; Sax, M.; Dömling, A. A new and efficient multicomponent solid-phase synthesis of 2-acylaminomethylthiazoles. *Tetrahedron Lett.* **2003**, *44*, 3679–3682.

(39) Kolb, J.; Beck, B.; Almstetter, M.; Heck, S.; Herdtweck, E.; Dömling, A. New MCRs: the first 4-component reaction leading to 2,4-disubstituted thiazoles. *Mol. Diversity* **2003**, *6*, 297–313.

(40) Kolb, J.; Beck, B.; Dömling, A. Simultaneous assembly of the β-lactam and the thiazole moiety by a new multicomponent reaction. *Tetrahedron Lett.* **2002**, *43*, 6897–6901.

(41) Dömling, A.; Beck, B.; Eichelberger, U.; Sakamuri, S.; Menon, S.; Chen, Q. Z.; Lu, Y.; Wessjohann, L. A. Total synthesis of tubulysin U and V. *Angew. Chem., Int. Ed.* **2007**, *46*, 2347–2348.

(42) Lau, H. H.; Schöllkopf, U. Synthesen mit α-metallierten isocyaniden, LII. Synthesen mit α-metallierten isocyaniden, LII. Synthese von 2-alkyl- und 2-acyl-1-methylimidazol-4-carbon-säuremethylestern aus (*Z*)-β-dimethylamino-α-isocyanacrylsäuremethylester und alkyl- oder acylhalogeniden. *Liebigs Ann. Chem.* **1982**, 2093–2095.

(43) Sandham, D. A.; Barker, L.; Beattie, D.; Beer, D.; Bidlake, L.; Bentley, D.; Butler, K. D.; Craig, S.; Farr, D.; Ffoulkes-Jones, C.; Fozard, J. R.; Haberthuer, S.; Howes, C.; Hynx, D.; Jeffers, S.; Keller, T. H.; Kirkham, P. A.; Maas, J. C.; Mazzoni, L.; Nicholls, A. Synthesis and biological properties of novel glucocorticoid androstene C-17 furoate esters. *Bioorg. Med. Chem.* **2004**, *12*, 5213–5224.

(44) Sabot, C.; Kumar, K. A.; Meunier, S.; Mioskowski, C. A convenient aminolysis of esters catalyzed by 1,5,7-triazabicyclo[4.4.0]dec-5-ene (TBD) under solvent-free conditions. *Tetrahedron Lett.* **2007**, *48*, 3863–3866.

(45) Nunami, K.; Yamada, M.; Fukui, T.; Matsumoto, K. A novel synthesis of methyl 1,5-disubstituted imidazole-4-carboxylates using 3-bromo-2-isocyanoacrylates (BICA). *J. Org. Chem.* **1994**, *59*, 7635–7642.

(46) Fehrentz, J. A.; Castro, B. An efficient synthesis of optically active α-(*t*-butoxycarbonylamino)-aldehydes from α-amino acids. *Synthesis* **1983**, 676–678.

(47) Bockbrader, K. M.; Tan, M.; Sun, Y. A small molecule Smac-mimic compound induces apoptosis and sensitizes TRAIL- and etoposide-induced apoptosis in breast cancer cells. *Oncogene* **2005**, *24*, 7381–7388.

(48) Oost, T. K.; Sun, C.; Armstrong, R. C.; Al-Assaad, A. S.; Betz, S. F.; Deckwerth, T. L.; Ding, H.; Elmore, S. W.; Meadows, R. P.; Olejniczak, E. T.; Oleksijew, A.; Oltersdorf, T.; Rosenberg, S. H.; Shoemaker, A. R.; Tomaselli, K. J.; Zou, H.; Fesik, S. W. Discovery of potent antagonists of the antiapoptotic protein XIAP for the treatment of cancer. *J. Med. Chem.* **2004**, *47*, 4417–4426.

(49) Spencer, R. W. High-throughput screening of historic collections observations on file size, biological targets, and file diversity. *Biotechnol. Bioeng.* **1998**, *61*, 61–67.

(50) Jacoby, E.; Boettcher, A.; Mayr, L. M.; Brown, N.; Jenkins, J. L.; Kallen, J.; Engeloch, C.; Schopfer, U.; Furet, P.; Masuya, K.; Lisztwan, J. *Chemogenomics*; Jacoby, E., Ed.; Methods in Molecular Biology, Vol. 575; Springer: Heidelberg, Germany, 2009; pp 173−194.

(51) Kussie, P. H.; Gorina, S.; Marechal, V.; Elenbaas, B.; Moreau, B.; Levine, A. J.; Pavletich, N. P. Structure of the MDM2 oncoprotein bound to the p53 tumor suppressor transactivation domain. *Science* **1996**, *274*, 948–953.

(52) Shuker, S. B.; Hajduk, P. J.; Meadows, R. P.; Fesik, S. W. Discovering high-affinity ligands for proteins: SAR by NMR. *Science* **1996**, *274*, 1531–1534.

(53) Goddard, T. D.; Kneller, D. G. *SPARKY*, version 3; San Francisco, CA.

(54) Rega, M. F.; Reed, J. C.; Pellecchia, M. Robust lanthanide-based assays for the detection of anti-apoptotic Bcl-2-family protein antagonists. *Bioorg. Chem.* **2007**, *35*, 113–120.

(55) Kangas, L.; Gronroos, M.; Nieminen, A. L. Bioluminescence of cellular ATP: a new method for evaluating cytotoxic agents in vitro. *Med. Biol.* **1984**, *62*, 338–343.